Shallow submarine mud volcano in the Northern Tyrrhenian sea, Italy

Anna Saroni, Alessandra Sciarra, Fausto Grassa, Andreas Eich, Miriam Weber, Christian Lott, Giacomo Ferretti, Roberta Ivaldi, Massimo Coltorti

PII: S0883-2927(20)30214-6

DOI: https://doi.org/10.1016/j.apgeochem.2020.104722

Reference: AG 104722

To appear in: *Applied Geochemistry*

Received Date: 24 April 2020

Revised Date: 4 July 2020

Accepted Date: 28 July 2020

Please cite this article as: Saroni, A., Sciarra, A., Grassa, F., Eich, A., Weber, M., Lott, C., Ferretti, G., Ivaldi, R., Coltorti, M., Shallow submarine mud volcano in the Northern Tyrrhenian sea, Italy, *Applied Geochemistry*, https://doi.org/10.1016/j.apgeochem.2020.104722.

Shallow submarine mud volcano in the Northern Tyrrhenian sea, Italy

Anna Saroni[a], Alessandra Sciarra[a,b], Fausto Grassa[c], Andreas Eich[d], Miriam Weber[d], Christian Lott[d], Giacomo Ferretti[a], Roberta Ivaldi[e], Massimo Coltorti[a,c]

a Department of Physics and Earth Sciences, University of Ferrara, Via Saragat 1, 44122, Ferrara, Italy
b Istituto Nazionale di Geofisica e Vulcanologia, Sezione Roma 1, via di Vigna Murata 605, 00143, Rome, Italy
c Istituto Nazionale di Geofisica e Vulcanologia, Sezione di Palermo, via Ugo La Malfa 153, 90146, Palermo, Italy
d HYDRA Marine Sciences GmbH, Burgweg 4, 76547, Sinzheim, Germany
e Istituto Idrografico della Marina, Ministero della Difesa, Passo dell'Osservatorio 4, 16134, Genova, Italy

Keywords: submarine emission, mud volcano, methane, gas geochemistry, Tyrrhenian sea.

ABSTRACT

Submarine methane emissions in the Tuscan Archipelago have been studied since the 1960s, both for economic and research purposes. Offshore gas seepage is mainly concentrated southward and westward of Elba island, along N-S faults related to recent extensional activity in the Tuscan shelf and N-S trending positive magnetic anomalies, which have been interpreted as serpentinites associated with ophiolitic rocks due to their very high magnetic susceptibility.

This study focuses on the gas chemistry of a new emission site corresponding to a shallow water mud volcano in the Scoglio d'Affrica area. The Scoglio d'Affrica seep has a gas composition typical of mud volcanoes, with methane as the prevalent component (95 vol%) and minor gases which include carbon dioxide, nitrogen and trace amounts of helium. The combined stable C and H isotope composition of CH_4 ($\delta^{13}C$ and $\delta^{2}H$) and the enrichment in heavy carbon isotopes of CO_2, highlight a prevalent secondary microbial origin for these fluids ($\delta^{13}C \sim -35.8$ ‰ vs VPDB; $\delta^{2}H \sim -166$ ‰ vs VSMOW; $\delta^{13}C_{CO2}$ up to + 21.7 ‰ vs VPDB). Thus, in spite of the occurrence of positive magnetic anomalies, a possible abiotic origin of methane is excluded. Moreover, the gas from the mud volcano is extremely depleted in ^{3}He and presents typical $^{3}He/^{4}He$ ratios of a geological setting in which radiogenic crustal helium is strongly predominant. A photo-mosaic of the mud volcano is also reported. A possible connection with other submarine methane emissions in the Tuscan Archipelago is limited to emissions located few kilometers from the Scoglio d'Affrica area. Recent emissions in the area suggest that gases similar in composition from distinct reservoirs, find their way to the surface from Eocene deposits in different time intervals and through different faults and fractures, placed along the Elba-Pianosa ridge.

1. Introduction

Mud volcanoes are formed in sedimentary basins as the surface expression of hydrocarbon migration (Dimitrov, 2002; Etiope, 2015). The combination of gas overpressure (high pore fluid pressure at great depth) and gravitative instability of shales (Niemann and Boetius, 2010; Mazzini and Etiope, 2017) may result in the migration, through faults or fissures, towards the surface of a multi-phase material called mud breccia. Mud breccia is made up of sediments, together with rock clasts coming from the different stratigraphic horizons through which the mud passes on its way to the surface, gas (mainly hydrocarbons), water (from brackish to brine composition), and occasionally oil. The mud discharge, fluidified by gas and water, creates cone shaped structures. Usually, there is not only a single isolated cone, but the mud volcano consists of a group of cones and crater systems (Mazzini and Etiope, 2017).

The prevalent compound of the gas released by mud volcanoes is usually methane, often above 80 vol%. Other minor gases are carbon dioxide (CO_2), nitrogen (N_2), alkanes (ethane to butane) and trace amounts of helium (He) (Milkov et al., 2003; Mazzini and Etiope, 2017). A global data set of analysed gas from onshore mud volcanoes show that they are mostly of thermogenic origin (about

76%), meaning that they are produced by thermal degradation of organic matter or oil cracking (catagenesis) in relatively deep sediments at temperatures typically up to 230–240 °C ($\delta^{13}C$-CH_4∼−46.4‰ VPDB - Vienna Pee Dee Belemnite, as average of 201 mud volcanoes; Etiope et al., 2009a).

Mud volcanism is a common phenomenon both onshore and offshore. Although the mechanism of formation, the tectonic setting, the products, the activity and the contribution to greenhouse effects of terrestrial mud volcanism have been clearly delineated from the early 1900s on (e.g. Goubkin and Fedorov, 1938), submerged mud volcanism has been characterized by practical and visual difficulties around sampling and identification. Hence, it is probable that a significant number of submarine mud volcanoes are still to be discovered. The literature regarding offshore mud volcanoes has expanded in the last decades thanks to the diffusion of side scan sonar, Remotely Operated Vehicles and the advances in sampling equipment. Several studies confirm their presence in the eastern and western Mediterranean Sea (Cita et al., 1981; Limonov et al., 1994; Ivanov et al., 1996; Akhmanov and Woodside, 1998; Milkov A. V., 2000; Bellaiche et al., 2001; Kopf et al., 2001; Zitter et al., 2005; Lykousis et al., 2009; Mascle et al. 2014) as a result of the convergence of the African and Eurasian plates. In this context, cold seeps and mud volcanism are predominant within the Mediterranean Ridge, in correspondence with the accretionary prism of the Hellenic Arc subduction zone, but they are also found along the Cyprus Arc, within the Nile deep-sea fan, in the Ionian sea and further west in the Gulf of Cadiz (Zitter et al., 2005; Rabaute and Chamot-Rooke, 2007; Dupré et al., 2008; 2010; Loher et al., 2018). However, in these geological contexts mud volcanism is found in deep water (more than 400 m water depth).

We found the shallowest mud volcano in the Mediterranean Sea near the Scoglio d'Affrica, which is located at about 7-12 m depth in the Thyrrenian sea (figure 1). Methane emissions in the Tuscan Archipelago had already been reported since the 1960s (Del Bono and Giammarino, 1968). The Italian oil company AGIP (Azienda Generale Italiana Petroli) carried out exploration projects of the site through two wells, Martina 1 and Mimosa 1, near Pianosa island and Scoglio d'Affrica area, revealing the presence of hydrocarbon gas in Early Miocene sand levels and in Eocene flysch formations. However, neither of the two wells were economically feasible to exploit and they were abandoned (Camera dei Deputati, 1984). More recently, two other shallow water cold seeps were discovered and studied for research purposes, one off the west coast of Elba island, near Pomonte (Ruff et al., 2016; Wiedling, 2010; Meister et al., 2018; Sciarra et al., 2019a) and the other one near Pianosa Island (Meister et al., 2018) (figure 1).

In Pianosa, gas emissions occur at 10 to 45 m water depth out of carbonate sand and rocky outcrops and there is no data about their chemical and isotope composition. On the contrary, Pomonte gas bubbles are escaping from sediments and sandy patches between seagrass beds. In this area, the released gas is methane dominant (CH_4 > 85 vol%) with a very low CO_2 content (< 1.5 vol%) and a helium isotope signature which indicates a non-negligible mantle derived component (Sciarra et al., 2019a). The main gas chemistry, the stable C and H isotopic compositions of CH_4 ($\delta^{13}C$-$_{CH4}$−18‰; $\delta^{2}H$-$_{CH4}$−141‰) and the reconstruction of the geological-structural setting of the Elba ophiolite sequence, suggest that the CH_4 is likely to be abiotic in origin and that it derives from a process of serpentinization in a continental ultramafic rock system (Sciarra et al., 2019a).

The seepages in Pomonte together with the emissions in the Scoglio d'Affrica are seen to be aligned as the N-S trending positive magnetic anomaly, found at the eastern margin of the Elba-Pianosa ridge, whereas Elba island marks a W-E oriented zone of magnetic lineations site. The positive anomalies could be linked to the ophiolitic suture zone, as Eriksson and Savelli (1989) suggested and as the Istituto Nazionale di Geofisica e Vulcanologia (INGV) expedition reported (INGV, July 2017).

This paper contains the first combined visual seafloor observations, sedimentology and facies analyses together with the chemical and isotope characterization on the fluids emitted from a mud

volcano in the Scoglio d'Affrica area, acquired during a research project in the summer of 2018. We present a photo mosaic of the mud volcano area, together with visual observations and data of gas, water, sediment and rock analyses. The synthesis of the gas geochemical data, compared with previous studies, evidences constraints on spatial and temporal variations of mud volcanism and sheds light on the gas origin together with possible links with other emission sites.

2. Geological setting

The geologic history of the Northern Tyrrhenian Sea is strictly linked to the Northern Apennine Orogeny, developed since the late Eocene as a consequence of the collision due to the closure of the Tethys Ocean (Carminati and Doglioni, 2012). After this collision, an extensive tectonic regime became predominant over time. This stretched inner part of the Apenninic orogenic belt allowed the opening of the Tyrrhenian Basin and the genesis and the rise of anatectic melts, due to the uplift of the asthenospheric mantle (Pandeli et al., 2013). Magmatic bodies developed in several islands in the Northern Tyrrhenian Sea, such as Capraia (between ~7.2 and ~4.8 Ma; Carminati and Doglioni, 2012), western and eastern Elba, Montecristo (~7.1 Ma; Carminati and Doglioni, 2012), and Giglio (~5 Ma; Carminati and Doglioni, 2012), forming the Tuscan Magmatic Province with the Tuscany mainland. The overall result of the crustal stretching in the Northern Tyrrhenian Sea produced uniformly oriented normal fault sets trending north-south and northwest-southeast (Keller and Coward, 1996 and references therein) that created several small Neogene sedimentary basins surrounded by structural ridges which characterize the Tuscan shelf (Pascucci et al. 1999). The most active zone tectonically is the Elba-Pianosa Ridge, which is a rising antiform, with a N-S axis that divides the Tuscan shelf from the Corsica basin, filled with about 8.5 km of Eocene to present sedimentary deposits (Mauffret et al. 1999).

The sampling area is part of the Elba-Pianosa Ridge. This mainly submarine structural high emerges to the surface at Pianosa Island and Scoglio d'Affrica and consists of a thick (more than 3,000 m) Eocene-Oligocene silicoclastic succession where the presence of gas localized in Eocene, Oligocene and Miocene turbiditic deposits was found in the 70s and 80s during the AGIP drilling projects. Pianosa island consists of Lower Miocene (Burdigalian) to Pleistocene shallow marine to continental deposits (Marina del Marchese, Golfo della Botte and Pianosa Formations; Cornamusini et al., 2002 and references therein), whereas Scoglio d'Affrica is composed of shallow marine organogenic limestones with a prevalent algal component and frequent malacofauna. These sediments are dated between the Pleistocene and Holocene, contemporary to the Tuscan Nappe (Motteran and Ventura, 2005). Two lithofacies were specifically identified, both related to high hydrodynamic environments: packstones-wackestones which correspond to a depositional environment of seashore, and coral lithofacies (grainstone), situated on top of the former (Motteran and Ventura, 2005). These sediments are sub-horizontal and lay in a transgressive sequence on the carbonate rocks of the Tuscan Nappe (Cornamusini et al., 2002). Cornamusini et al. (2002) also suggest that the islet is bordered by high angle normal faults, which were active during post-Burdigalian time. Regarding the seafloor around Scoglio d'Affrica, morphological terraces, faults and methane activity had already been reported by Barletta et al. (1969).

3. Methods

3.1 Gas sampling and analysis

Gas samples were collected in July 2018 by SCUBA diving by placing open bottles at the top of the mud cones or the fractured rock, in correspondence to the bubble emissions. The gas was stored in 100 mL glass bottles after water displacement. A total of 4 sites, from the same area were sampled.

Permanent gases (He, H_2, O_2, N_2, CO, CH_4 and CO_2) were measured by means of a gas chromatograph (GC, Agilent 7890 equipped with PPU and MS5A columns) associated with a MicroGC module (equipped with a PPU column) and a double detector (TCD and FID) using argon as carrier gas. Higher hydrocarbons (C_2-C_5) were analyzed using a Shimadzu 2010 GC equipped with FID and a capillary CP Poraplot column (Q 25 m, 0.25 i.d.) using helium as carrier gas. The column temperature was programmed to start at 25°C for 4 min and then increased by 5°C/min up to 180°C, where it remained for 5 min. Analytical precision for GC analyses is better than ±5% for trace gases and ±10% for alkanes. Stable carbon and hydrogen isotope compositions of CH_4 and CO_2 were measured using a Delta Plus XP IRMS coupled with a Thermo TRACE GC and a Thermo GC/C III interface and equipped with a Poraplot column (Q 25 m, 0.32 i.d.). The column temperature was isothermal at 50°C. An in-house reference gas (δC_1=-49.5±0.3‰, δD=-200±2.5‰; CH_4 grade 6.0 i.e. 99.9999%) calibrated against H-Iso reference (SCOTT 2500 ppm, δC_1=-23.9±0,3‰, δD=-156±5‰) and BIO (SCOTT 2500 ppm, δC_1=-68.6±0.3‰, δD=-240±5‰) was used for isotopic standards. $^{13}C/^{12}C$ ratios are reported as $\delta^{13}C$ values (1 σ=0.1‰) against VPDB standard and $^{2}H/^{1}H$ ratios are reported as $\delta^{2}H$ values (1σ=1‰) against VSMOW standard. Helium isotope composition (expressed as R/Ra, which is $^{3}He/^{4}He$ of the sample versus the same $^{3}He/^{4}He$ ratio in atmosphere, Ra=1.386×10^{-6}) and ^{20}Ne content were analyzed by a GVI Helix SFT mass spectrometer.

All the chemical and isotope analyses on gas samples were carried out at INGV-Palermo laboratories.

3.2 Sediment, rock and water sampling and analysis

Sediment samples were taken using plastic corers and plastic bags. The cores were driven to a depth of about 30 cm into the mud cones by hand. The upper part was then closed using a rubber stopper with a hole for pressure balance. Surrounding sediment was carefully removed to close the bottom end with a second rubber stopper. The sampled cores were then opened and the sediment split into three sections corresponding to three different depths and collected into plastic bags and plastic bottles. Sediment samples were stored at 5 °C until further analysis. Two different methods of grain size analysis were used: sieving and X-ray sedimentation analysis. The first one was used for coarse-grained sediment (≥63 µm), whereas X-ray sedimentation technique was performed for the fine-grained part of the samples (<63 µm) using Micromeritics SediGraph 5100.

Rock samples were taken using hammer and chisel from blocks and clasts at the seabed close to the emission site. Thin sections were prepared and analyzed by a polarization microscope to define the rock type.

Porewater samples were taken using Rhizon membranes attached to syringes. The membrane was inserted into the ground to about 4 cm depth. Seawater samples, instead, were taken using plastic bottles and syringes. Electrical conductivity (EC) values were read using a RS 180-7127 Conductivity Meter after adopting a dilution factor of 100 using Milly-Q water (Millipore USA). Anions were determined by an ion chromatographer with an isocratic dual pump (Dionex ICS-1000) equipped with an AS9-HC 4x250 mm high-capacity column and an AERS 500 4-mm suppressor. An AS-40 Dionex auto-sampler was employed to run the analysis. Sodium carbonate (9 milliMol) was used as eluent with a flow rate of 1 mL/min. Standards were prepared from the stocked solution (Dionex Seven Anion Standard II in deionized water) adopting a serial dilution of 1, 2, 10 and 100 factors. Blank sample was prepared using Milly-Q water. Main cations and trace elements were measured using a X-Series Thermo-Scientific spectrometer (ICP-MS). Specific amount of Rh and Re were added to the analyzed solutions as internal standard, in order to correct the instrumental drift.

Sediment, rock and water samples analysis were carried out at the University of Ferrara, Department of Physics and Earth Sciences.

4. Results

4.1 Visual seafloor observations

The area near the two previous expeditions (HYDRA, 2011; INGV, March 2017) was explored by research divers from the University of Ferrara and the HYDRA Institute in collaboration with the Capitaneria di Porto of Portoferraio in July 2018. During the 2018 exploration, emission activity was very low in the south shoal (2017 site), whereas no signs of emissions were found in the north shoal (2011 site); however, another emission point was discovered between these two sites. It corresponds to a shoal about 5 km north-east of Scoglio d'Affrica, which is dominated by blocks and clasts alternated to muddy sediment located in correspondence to the emissions. All these three emission sites correspond to three different morphological levels of about 7-10 m depth. Active mud volcanic areas were identified from *in situ* observations by geological characteristics of fresh mud eruption or visible fluid and gas emissions (at least 10 emission points were identified, shown in figure 2). The gas was emitted in big bubbles (10-15 cm) from conical mud mounds or from bubbles of mm- to cm-size from sandy-muddy sediment or fissures in the blocks as a peripherical discharge (figure 3).

4.2 Gas chemistry

The general gas chemistry of these submarine emissions is quite similar to those of the terrestrial mud volcanoes summarized by Etiope et al. (2009a). The results are reported in table 1. The prevalent gas component is methane ranging from 95.5 to 96.82 vol%. Other gases include carbon dioxide (from 0.97 to 1.30 vol%), nitrogen (from 0.41 to 0.84 vol%), ethane (0.026–0.036 vol%) and helium (up to 0.0046 vol%). The $CH_4/(C_2H_6+C_3H_8)$ ratio ranges from ~2670 to ~3700, highlighting very high values relative to most thermogenic gas. Low C_1/C_{2+} ratios ($<10^3$) are a definite indication of thermogenic hydrocarbon contributions to the fluids, whereas higher C_1/C_{2+} ratios ($>10^3$) do not rule out the involvement of thermogenic hydrocarbons (Bernard et al., 1978; Kim et al., 2012). The isotopic composition of CH_4 between samples varies in a narrow range, from −163 to −168‰ vs VSMOW for $\delta^2H\text{-}_{CH4}$ and from −34.9 to −36.8‰ vs VPDB for $\delta^{13}C_{CH4}$. CO_2 is strongly-enriched in heavy carbon isotopes with $\delta^{13}C_{CO2}$ ranging from +15.3 to +21.7‰ vs VPDB. The $^3He/^4He$ ratios, normalized to the same ratio in the atmosphere (denoted as $Ra=1.39\cdot10^{-6}$ Mamyrin et al., 1970; Clarke et al., 1976; Sano et al., 2008; Mabry et al., 2013) are identical in all the collected gas seeps and equal to 0.01 Ra. The $^4He/^{20}Ne$ ratios, spanning from 75 to ~330, are at least two orders of magnitude higher than that of air ($^4He/^{20}Ne=0.318$, Sano & Wakita, 1985) thus indicating a negligible contribution from atmospheric gas. The $CH_4/^3He$ ratios range from $1.24\cdot10^{12}$ to $1.76\cdot10^{12}$.

4.3 Petrography

Mudstone samples showed a very fine matrix with vuggy microporosity, microfossils and veins of calcite. Crystals were not distinguishable in the groundmass. The porosity could be secondary due to fossil and grain dissolution. Fossils were not easy to identify, because of the alteration and the poor preservation of the sample. Nevertheless, some single valves were recognizable, possibly bivalves, and also some globular forms. These last ones showed trochospiral tests and globular inflated chambers, typical of the *Globigerinidae*, a family of planktonic foraminifera. Their biostratigraphic distribution ranges from Paleocene to nowadays.

Siltite samples showed a very thin (micrometric) groundmass interrupted by several millimetric veins of calcite and of quartz in minor quantity. Calcite and quartz crystals were allotriomorphic and anhedral. The texture of the rock consisted of sub-parallel, wavy to crenulated laminations on micrometric scale. In the matrix it was possible to distinguish some quartz and oxide minerals.

4.4 Grain size analysis of the extruded sediment

The extruded sediment was characterized by a wide range of grain sizes. According to the guide lines for the granulometric analysis of marine sediments deliberated by Sistema Nazionale per la Protezione dell'Ambiente (SNPA) in 2018 (Romano et al., 2018), Shepard's diagram (1954) was considered for the classification of samples with <20% of gravel, where gravel is incorporated to sand percentage (figure 4A). Samples that had more than 20% of gravel, were classified using a modified Shepard's diagram, where silt and clay are put together (figure 4B). According to this classification, it was possible to identify silty clay, sand-silt-clay and gravelly mud sediments (table 2).

4.5 Porewater and seawater chemistry

In the mud volcano area, porewater and seawater samples did not show significant differences from the water samples taken outside the area. The pH was around 8.00 and salinity was about 38 PSU. Porewater samples showed an enrichment in B (6.34 and 11.55 mg/l) compared to samples taken outside the mud volcano area (~4.35 mg/l). B is a typical element that derives from fluid–rock interaction (Mazzini et al., 2009; Hensen et al., 2015); in the marine environment, its enrichment can derive from clay dehydration (Palmer et al., 1987; Barth, 1997). The results are shown in table 1S, 2S and 3S in the supplementary material.

5. Discussion

5.1 Gas origin

The gas chemistry of the collected samples is typical of mud volcanoes (Etiope et al., 2009b), with methane as the prevalent gas component (>95 vol%) and minor gases which include carbon dioxide, nitrogen and heavier alkanes and helium, whereas CO is present in trace amounts. In order to assess the origin of the hydrocarbon gases, the stable isotopes as well as the molecular composition have been successfully used in several geological contexts. $\delta^{13}C_{CH4}$ values from -30‰ to -50‰ are interpreted as thermogenic gases, given that as source rocks become more thermally mature, they expel C_1 relatively enriched in ^{13}C. Thermogenic gases are also characterized by $C_1/(C_2+C_3)$ ratios (the so-called Bernard parameter) lower than 50. On the contrary, very early mature thermogenic gases have $\delta^{13}C_{CH4}$ from -55‰ to -73‰ (Milkov and Etiope, 2018), thus significantly overlapping with the $\delta^{13}C_{CH4}$ values of the primary microbial gases ($\delta^{13}C\text{-}_{CH4}$< -50‰). Microbially produced hydrocarbons can be distinguished from very early mature thermogenic gas because of their Bernard ratios from 10^3 to 10^5.

The $\delta^{13}C_{CH4}$ values of the analyzed gas have an average of ~-35.8‰, which is in the range of ^{13}C values for thermogenic gas, whereas the Bernard parameter (between 2676 and 3687) is typical for microbial-produced gas. The CH_4 isotope data and the Bernard ratio are also potentially consistent with the oxidation of microbial methane; however, oxidation usually implies extreme enrichment of carbon and hydrogen in heavy isotopes (reaching values of $\delta^{13}C$ and $\delta^{2}H$ as high as +45‰ and +301‰; Milkov and Etiope, 2018). Moreover, bacterial consumption of CH_4 appears to proceed at a significantly greater rate than for hydrocarbon gases with higher molecular weight, such as ethane and propane; the result is a decrease of the $C_1/(C_2 + C_3)$ ratio from values of 10^3 and 10^5, with the possibility of reaching values of less than 10 (Whiticar, 1999; Milkov and Etiope, 2018). The $C_1/(C_2 + C_3)$ ratio higher than 2600 could be explained as follows: i) a molecular fractioning occurring during migration of a thermogenic gas that may increase the $C_1/(C_2+C_3)$ ratio while the isotopic composition of C_1 remains unaltered (Etiope et al., 2009b), or ii) as the result of microbial

degradation during the biodegradation of liquid hydrocarbons to methane (James and Burns, 1984; Jay Katz, 2011).

In the most common genetic diagrams, such as $\delta^{13}C_{CH4}$ vs $C_1/(C_2+C_3)$ (Bernard et al., 1977: figure 5A) and $\delta^{13}C_{CH4}$ vs δD_{CH4} (Schoell, 1983; Whiticar et al., 1986; figure 5C and figure 6), which have been recently revised by using a larger global dataset (Milkov and Etiope, 2018), the collected gases fall in the field between late mature thermogenic gas (LMT) and secondary microbial gas (SM), suggesting a possible mixture of the two components. However, the $\delta^{13}C_{CO2}$ values highlight that microbial processes are strongly predominant (figure 5B). The $\delta^{13}C_{CO2}$ values span from +15.3 to +21.7‰ vs V-PDB. They fall far from the typical values found either in mantle-derived fluids ($\delta^{13}C_{CO2}$ in MORB – Mid Ocean Ridge Basalts – from –8 to –4‰ vs VPDB; Des Marais & Moore, 1984; Marty et al., 1989; Sano and Williams, 1996) and in crustal gas originated from thermo-metamorphic reactions ($\delta^{13}C_{CO2}$ from −2 to +2‰ vs VPDB; Sano and Marty, 1995). Moreover, such unusual extremely ^{13}C-rich values are heavier than the carbon isotope signature of CO_2 associated to late mature thermogenic gas (LMT; figure 5B; Shuai et al., 2013). CO_2 enriched in heavy carbon isotopes is very often associated to secondary microbial methanogenesis following hydrocarbon biodegradation. The residual CO_2 deriving from the biodegradation of methane has $\delta^{13}C_{CO2}$ generally exceeding +2‰ (Milkov, 2018) which may reach values up to +36‰ (Tassi et al., 2012).

All the gases collected in the Scoglio d'Affrica area fall into the secondary microbial origin region (figure 5B), far from the nearby Pomonte gases, which clearly show abiotic origins. Secondary microbial gases (mainly CH_4) are made by microbes during oil biodegradation (they represent the end result of biodegradation) and are usually mixed with oil-associated biodegraded thermogenic gas. A huge increase in ^{13}C of CO_2 such as in the Scoglio d'Affrica samples is almost never observed in gases of other origins (Milkov and Etiope, 2018). Therefore, the molecular and isotope composition of hydrocarbons seems to indicate that i) the secondary processes (biodegradation), which may have altered the pristine molecular gas composition, are the main methanogenic processes in the Scoglio D'Affrica seeps and ii) the thermal degradation of organic matter is considered as a minor process.

The composition of the gas sampled in 2018 is well comparable to the gas sampled by the HYDRA Institute in 2011 (figure 5) and reported in Meister et al. (2018) from a site located about 1 km to the north from the Scoglio d'Affrica sampling area. The gases released from these two areas are likely to be fed by two separate reservoirs having a homogeneous chemical and isotope composition rather than by the same gas reservoir.

The helium isotopes are powerful natural tracers which allow us to distinguish the origins of the three main reservoirs on Earth (mantle, crust and atmosphere; Ozima and Podosek, 2002). ^3He is mainly primordial in origin, originating from mantle degassing or from Air-Saturated Water (ASW) trapped in the pores and minerals. By contrast, ^4He is essentially produced by the decay of U and Th in the continental crust. This results in $^3He/^4He$ ratios close to 8±1 Ra (Kurz et al., 1982) in the upper mantle (MORB-type) whereas the continental crust is characterized by $^3He/^4He$ ratios in the range between 0.01 and 0.05 Ra (Morrison and Pine, 1955).

The samples collected at Scoglio d'Affrica are extremely depleted in ^3He, with $^3He/^4He$ ratios values of 0.01 Ra. These values are usually found in gas emitted from a geological setting in which radiogenic crustal helium is strongly predominant, as several studies of noble gases from other mud volcanoes and hydrocarbon-related fluids confirm (e.g. $^3He/^4He$ ratios values ranging from 0.03 to 0.05 Ra in Ballentine and O'Nions (1994); from 0.01 Ra in Lavrushin et al. (1996); from 0.02 Ra in Kopft et al. (2003); from 0.02 to 0.17 Ra in Battani et al. (2010); from 0.03 to 0.05 Ra in Zheng et al. (2017); from 0.01 to 0.1 Ra in Nuzzo et al. (2019); from 0.02 to 0.03 Ra in Sciarra et al. (2019b)). On the contrary, a mantle contribution corresponds to higher $^3He/^4He$ ratios values (e.g.

values up to 1.4 Ra in Lavrushin et al. (1996) and in Kopft et al. (2003); from 0.4 to 1.9 Ra in Yang et al. (2003); up to 1.60 Ra in Lavrushin et al. (2009)). Therefore, these values suggest that the tectonic discontinuities which drive mud volcanism in the Scoglio d'Affrica area are not deeply rooted but rather limited to shallow crustal levels (Caracausi et al., 2005; Caracausi and Paternoster, 2015). Moreover, it seems that a possible ^{3}He contribution directly released from mantle or from remnant magmatic sources (e.g. a magmatic intrusion) can be excluded, whereas it occurs in the case of the nearby Pomonte seeps. In this latter area, Sciarra et al. (2019a) estimated a mantle-derived helium component from 10 to 30% likely due to the degassing of the Monte Capanne pluton on the western sector of Elba Island (figure 7A).

The $CH_4/^{3}He$ ratio is another effective parameter to discriminate the abiotic component of the gas; values from 10^{12} to 10^{13} are consistent with biogenic and crustal contributions (Wakita et al., 1990; Sakata et al., 1997), whereas abiotic methane in hydrothermal systems can reach values of 10^{6} (Sano et al., 2017). The average molecular ratio of CH_4 to ^{3}He in the Scoglio d'Affrica samples is $\sim 1.55 \cdot 10^{12}$, which definitely excludes an abiotic origin of the gas. On the other hand, the Pomonte gases show a $CH_4/^{3}He$ ratio of $\sim 1.92 \cdot 10^{9}$, confirming the presence of an abiotic component (figure 7B).

5.2 Relations between local geology and gas emissions

Regarding the lithology, the siltites and the marly mudstones found in the sampling area are different from the shallow marine organogenic limestones of Scoglio d'Affrica islet; therefore, the possibility that the fragments of rock found in the mud volcano area could derive from erosional processes of the islet was discarded. In relation to the siliciclastic succession of Eocene-Oligocene strata found in Martina 1 and Mimosa 1 wells by AGIP, four depositional units are identified in literature (figure 8), all separated by unconformities recognized by truncation in seismic stratigraphic analysis (Cornamusini et al., 2002; Cornamusini and Pascucci, 2014). According to Cornamusini and Pascucci (2014), who reported a detailed description of the depositional units, the more superficial lithology consists of Pleistocene deposits, mainly hybrid siliciclastic sandy-clay of shallow marine environment, which differs from the fragments found around the mud volcano. The other units, instead, contain mudstones and siltstones at several depths.

Moreover, the bathyal up to neritic environments that characterize these units are consistent with the microfossils found in the mudstones. The recognized microfossils are in fact attributable to the *Globigerinidae* family, which are planktonic foraminifera that commonly proliferate in pelagic environments. Biostratigraphic distribution of these microfossils spans from the Paleocene to nowadays and they can actually thrive at the latitude of the sampling area. Nonetheless, these foraminifera are commonly abundant only in deep sea sediments, whereas they are very rare or even absent in neritic sediments and in water shallower than 10 m such as those of the sampling area. The possibility that they were transported by stream flows from bathyal environments is not consistent with the high-energy condition of the investigated area and with the fine muddy matrix of the sample. Therefore, it is more likely that these globigerinids were deposited in more ancient sediments typical of deeper environments (bathyal) such as those of the Sub2 Unit of Mimosa 1 well. Unfortunately, the conservation state of the fossils prevents further in-depth classification, thus it was neither possible to date them nor correctly and consistently correlate them with the Unit of the mentioned wells. Although magnetic and gravimetric data of very high magnetic susceptibility are found in the Scoglio d'Affrica area, as they are found offshore in western Elba, the interpretation of this data as ophiolitic bodies (Eriksson and Savelli, 1989; Cassano et al., 2001; Caratori Tontini et al., 2004) is not supported by the stratigraphic sequences.

The geological setting of the mud volcano area suggests a possible correlation between methane reservoirs discovered by AGIP and the recent emissions. According to the temperatures from the Martina 1 deep exploration well, located ~14 km north of Scoglio d'Affrica, the estimated local

geothermal gradient is about 32 °C/km (GeoThopica: figure 1S). Thermal degradation of organic matter or oil cracking (catagenesis) in relatively deep sediments occurs at temperatures >60 °C, which in this case, correspond to a depth >1650 m. In line with the stratigraphical reconstruction reported by Cornamusini and Pascucci (2014) and assuming a secondary microbial origin of the gas, it is conceivable to infer that Eocene deposits are responsible of the process of methanogenesis. Moreover, the presence of hypothetical faults reported in literature (Pascucci et al., 1999; Cornamusini and Pascucci, 2014) could justify the rising of fluids to the surface.

6. Conclusions

Based on the morphology as well as the sedimentary, petrographic and geochemical characteristics of the solid materials together with the fluids expelled from the Scoglio d'Affrica site, these seeps can be classified as a mud volcano. The investigated area revealed three main active mud volcano sites, which showed seepage in 2011, 2017 and 2018. All these areas are characterized by the occurrence of conical-round morphologies at a shallow water depth (from 7 to 12 m) well distinguished from the seafloor which in turn is characterized by the presence of blocks and mud. The gas is emitted as large bubbles (up to 15 cm in diameter) from conical mud mounds or from centimeter to millimeter size bubbles from sandy-muddy sediment or fissures in the blocks as a peripherical discharge or during a dormant phase. The extruded sediment is characterized by a wide range of grain sizes, including mud.

All three sites, together with the gas found in the AGIP wells in the 70s, show the same gas composition, with methane as the prevalent gas component (>95 vol%) and minor gases which include carbon dioxide, nitrogen and little amounts of helium. Molecular and isotopic compositions of samples collected in 2011 and in 2018 point to a predominant secondary microbial origin of the methane ($\delta^{13}C$ mean around -35.7 ‰ vs. VPDB, positive $\delta^{13}C_{CO2}$ values up to + 21.7 ‰ vs. VPDB and Bernard ratios around 3000). $^{3}He/^{4}He$ ratios, which were determined for the first time in the samples collected in 2018, show typical values for a gas crustal emitted from a geological setting in which the radiogenic helium component is strongly dominant. Moreover, the contribution of deep magmatic fluids, as well as a ^{3}He component derived from the degassing of intruded magmatic bodies, can be ruled out.

The geological and stratigraphic reconstruction of the mud volcano area revealed the presence of lithologies that are also found in the clasts discovered within the mud breccias, with planktonic foraminifera that are commonly found in deep sea sediments. Based on the lithostratigraphic reconstructions and the local geothermal gradient, the source rocks can be identified in the Eocene deposits at a depth greater than 1700 m. On the contrary, the reconstruction of the geology does not identify the ophiolitic bodies that are considered responsible for the offshore magnetic anomalies in western Elba.

Finally, considering the depth of the gas source, the geological setting and the main chemical and isotope composition of the gas, which is similar to the samples collected in 2011, the Scoglio d'Affrica emissions are not comparable to those of the Pomonte seeps. Methane from Scoglio d'Affrica has a clear secondary microbial origin and helium is entirely produced within the crust from a radiogenic decay, whereas the Pomonte gas is characterized by shallow cold seeps of abiotic methane with a non-negligible mantle-derived ^{3}He-rich component (Sciarra et al., 2019a).

Acknowledgments

Authors are indebted to Capitaneria di Porto of Portoferrario, in particular Alessandro Guerra, Gilberto Cesaretti, Ruggiero Agripino and Domenico Castro for their support during the sampling campaign. Thanks are also due to two anonymous referees and to the editor for the constructive criticism and suggestions, which greatly improved the first version of the manuscript.

References

Akhmanov G. G. and Woodside J. M. (1998). Mud volcanic samples in the context of the Mediterranean Ridge mud diapiric belt. In: Robertson A. H. F., Emeis K. C., Richter C. and Camerlenghi A. (eds.). *Proceedings of the ODP, Scientific Results,* 160: College station, TX (Ocean Drilling Program), pp. 597-605.

Ballentine C. J. and O'Nions R. K. (1994). The use of natural He, Ne and Ar isotopes to study hydrocarbon-related fluid provenance, migration and mass balance in sedimentary basins. Geological Society London Special Publications Geofluids, v. 78, p. 347–361.

Barletta S., Del Bono G.L., Salvati L. (1969). Nota preliminare sui lavori geomorfologici e geominerari subacquei effettuati dal Servizio Geologico d'Italia dal 1964 al 1969. *Boll. Serv. Geol. It. CX*, 83-89.

Barth S. (1997). Boron isotopic analysis of natural fresh and saline waters by negative thermal ionization mass spectrometry. *Chemical Geology, 143*, 255-261.

Battani A., Prinzhofer A., Deville E. (2010). Trinidad mud volcanoes: The origin of the gas. In: L. Wood (ed.). *Shale tectonics: AAPG Memoir* 93, pp. 225 – 238.

Bellaiche G., Loncke L., Gaullier V., Mascle J., Courp T., Moreau A., Radan S., Sardou O. (2001). Le cone sous-marin du Nil et son réseau de chenaux profonds; nouveaux résultats (campagne Fanil). *Comptes Rendus de l'Academie des Sciences, Serie II. Sciences de la Terre et des Planètes 333/7*, 399-404.

Bernard B., Brooks J. M. Sackett, W. M. (1977). A geochemical model for characterization of hydrocarbon gas sources in marine sediments. *9th Annual OTC Conference, 2934*, 435–438.

Bernard B.B., Brooks J.M., Sackett W.M. (1978). Light-hydrocarbons in recent Texas continental-shelf and slope sediments. *J. Geophys. Res.-Oceans, 83*, 4053–4061.

Blumenberg M., Pape T., Seifert R., Bohrmann G. & Schlömer S. (2018). Can hydrocarbons entrapped in seep carbonates serve as gas geochemistry recorder? *Geo-Mar Lett, 38*, 121-129. https://doi.org/10.1007/s00367-017-0522-6.

Camera dei Deputati. Resoconto stenografico. IX Legislatura, 185° Seduta, 24 settembre 1984. http://www.legislature.camera.it (01/09/2017).

Caracausi A., Favara R., Italiano F., Nuccio, P. M., Paonita, A., & Rizzo, A. (2005). Active geodynamics of the central Mediterranean Sea: Tensional tectonic evidences in western Sicily from mantle□derived helium. *Geophysical Research Letters, 32*, L04312.

Caracausi, A. and Paternoster, M. (2015). Radiogenic helium degassing and rock fracturing: A case study of the southern Apennines active tectonic region. *Journal of Geophysical Research: Solid Earth, 120*, 2200–2211.

Caratori Tontini F., Stefanelli P., Giori I., Faggioni O., Carmisciano C. (2004). The revised aeromagnetic anomaly map of Italy. *Ann. Geophys., 47.*

Carminati E. and Doglioni C. (2012). Alps vs. Apennines: The paradigm of a tectonically asymmetric Earth. *Earth-Science Reviews, 112*, 67-96.

Cassano E., Anelli, L. Cappelli, V. Giori I., La Torre P. (2001). The Island of Elba - northern Tyrrhenian sea aeromagnetic and gravity data. *Ofioliti, 26,* 153–160.

Chiocci F. L., Casalbore D., Martorelli E., Beaubien S., Bigi S., Pierdomenico M. (2017). Emissioni di fluidi al largo dello scoglio d'Affrica (Arcipelago Toscano). Rapporto per il Dipartimento di Protezione Civile.

Cita M. B., Ryan W. B. F., Paggi L. (1981). Prometheus mud breccia: an example of shale diapirism in the Western Mediterranean Ridge. *Ann. Géol. Pays Hellén., 30,* 543–570.

Clarke W. B., Jenkins W. J., Top, Z. (1976). Determination of tritium by mass spectrometric measurement of ^{3}He. *International Journal of Applied Radiation and Isotopes, 27* (9), 515–522.

Cornamusini G., Lazzarotto A., Merlini S., Pascucci V. (2002). Eocene-Miocene evolution of the north Tyrrhenian Sea. *Boll. Soc. Geol. It., Volume Speciale n. 1,* 769-787.

Cornamusini G., Pascucci V. (2014). Sedimentation in the Northern Apennines–Corsica tectonic knot (Northern Tyrrhenian Sea, Central Mediterranean): offshore drilling data from the Elba–Pianosa Ridge. *International Journal of Earth Sciences, 103,* 821-842.

Del Bono G.L. and Giammarino S. (1968). Rinvenimento di manifestazioni metanifere nelle Praterie a Posidonie sui fondi marini prospicienti lo «Scoglio d'Africa» nell'Arcipelago Toscano. *Atti Ist. Geol. Univ. Genova, VI* (1), 11.

Des Marais D.J., Moore J.G. (1984). Carbon and its isotopes in mid-oceanic basaltic glasses. *Earth Planet. Sci. Lett., 69,* 43-57.

Dimitrov L. I. (2002). Mud volcanoes–the most important pathway for degassing deeply buried sediments. *Earth. Sci. Rev. 59,* 49–76.

Dupré S., Buffet G., Mascle J., Foucher J.-P., Gauger S., Boetius A., Marfia C., The AsterX AUV Team (2008). High-resolution mapping of large gas emitting mud volcanoes on the Egyptian continental margin (Nile Deep Sea Fan) by AUV surveys. *Mar. Geophys. Res., 29,* 275–290.

Dupré S., Woodside J., Klaucke I., Mascle J., Foucher J.-P. (2010). Widespread active seepage activity on the Nile Deep Sea Fan (offshore Egypt) revealed by high-definition geophysical imagery. *Mar. Geol., 275* (1/4), 1–19.

Eriksson L. and Savelli C. (1989). Magnetic anomalies and magmatic events in and around the island of Elba (Northern Tyrrhenian Sea). *Marine Geology, 87,* 85-93.

Etiope G. (2017). Abiotic methane in continental serpentinization sites: an overview. *Procedia Earth Planet. Sci. 17,* 9–12.

Etiope G. (2015). Natural Gas Seepage – The Earth's Hydrocarbon Degassing. Springer, pp. 199.

Etiope G., Feyzullayev A., Baciu C. L. (2009a). Terrestrial methane seeps and mud volcanoes: a global perspective of gas origin. *Mar. Pet. Geol., 26,* 333–344.

Etiope, G., Feyzullayev, A., Milkov, A.V., Waseda, A., Mizobe, K., Sun, C.H. (2009b). Evidence of subsurface anaerobic biodegradation of hydrocarbons and potential secondar methanogenesis in terrestrial mud volcanoes. *Mar. Pet. Geol., 26,* 1692–1703.

Etiope G. and Schoell M. (2014). Abiotic gas: atypical but not rare. *Elements, 10,* 291–296.

Etiope G., Samardžić N., Grassa F., Hrvatović H., Miošić N., Skopljak F. (2017). Methane and hydrogen in hyperalkaline groundwaters of the serpentinized Dinaride ophiolite belt, Bosnia and Herzegovina. *Appl. Geochem. 84*, 286–296.

GeoThopica. Banca Nazionale dei Dati Geotermici a cura del CNR – Istituto di Geoscienze e Georisorse ed in collaborazione con ENI S.p.A. http://palici.igg.cnr.it/wm_geothopica/map.phtml?winsize=large&language=it&config= (accessed 28 March 2020).

Goubkin I.M., Fedorov S.F. (1938). Mud Volcanoes of the Soviet Union and Their Connection with the Genesis of Petroleum Fields in Crimean-Caucasus Geologic Province. USSR Academy of Science, Moscow (in Russian).

Hensen C., Scholz F., Nuzzo M., Valadares V., Gràcia E., Terrinha P., Liebetrau V., Kaul N., Silva S., Martínez-Loriente S., Bartolome R., Piñero E., Magalhães V. H., Schmidt M., Weise S. M., Cunha M., Hilario A., Perea H., Rovelli L., Lackschewitz K. (2015). Strike-slip faults mediate the rise of crustal-derived fluids and mud volcanism in the deep sea. *Geology, 43* (4), 339–342.

HYDRA Institut für Meereswissenschaften (2011). Extract of expedition logbook Scoglio d'Africa/Formiche di Montecristo (unpublished).

INGV (March 2017). Relazione di sintesi sulle indagini svolte a seguito delle violente emissioni gassose nel tratto di mare tra le isole di Montecristo e Pianosa.

INGV (July 2017). Attività di prospezione geofisica e oceanografica su Nave Aretusa (IIM- Marina Militare) nel tratto di Mare tra le isole di Montecristo e Pianosa (Scoglio d'Africa). Rapporto tecnico.

Ivanov M. K., Limonov A. F., van Weering Tj. C. E. (1996). Comparative characteristics of the Black Sea and Mediterranean Ridge mud volcanoes. *Marine Geology, 132*, 253-271.

James A.T., Burns B.J. (1984). Microbial alteration of subsurface natural gas accumulations. *American Association of Petroleum Geologists Bulletin, 68*, 957–960.

Jay Katz B. (2011). Microbial Processes and Natural Gas Accumulations. *The Open Geology Journal, 5*, 75-83.

Keller J. V. A. and Coward M. P. (1996). The structure and evolution of the Northern Tyrrhenian Sea. *Geological Magazine, 133* (1), 1-16.

Kim J.-H., Torres M.E., Choi J.Y., Bahk J.J., Park M.H., Hong W.L. (2012). Inferences on gas transport based on molecular and isotopic signatures of gases at acoustic chimneys and background sites in the Ulleung Basin. *Org. Geochem., 43*, 26–38.

Kopf A. and Behrmann J. N. (2001). Extrusion dynamics of mud volcanoes on the Mediterranean Ridge accretionary complex. In: Vendelille B. C., Mart Y. and Vigneresse J. L. (eds.). *Salt, shales and igneous diapirs in and around Europe* (Vol. 174) (pp. 169-204). London: Geological Society of London, Special Publications.

Kopf A., Deyhle A., Lavrushin V.Y., Polyak B.G., Buachidze G.I., Eisenhauer A. (2003). Isotopic evidence for deep gas and fluid migration from mud volcanoes in a zone of incipient continental collision (Caucasus, Russia). *Int. J. Earth Sci., 92*, 407-426.

Kurz M. D., Jenkins W. J., Schilling J. G., Hart S. R. (1982). Helium isotopic variations in the mantle beneath the central North Atlantic Ocean. *Earth Planet Sci. Lett., 58*, 1–14.

Lavrushin V.U., Polyak B.G., Prasolov R.M., Kamenskii I.L. (1996). Sources of material in mud volcano products based on isotopic, hydrochemical, and geological data. *Lithol. Miner. Resour., 31* (6), 557-578.

Lavrushin V. Yu., Polyak B. G., Pokrovskii B. G., Kopp M. L., Buachidze G. I., Kamenskii I. L. (2009). Isotopic–Geochemical Peculiarities of Gases in Mud Volcanoes of Eastern Georgia. *Lithology and Mineral Resources, 44* (2), 183–197.

Limonov A. F., Woodside J., Ivanov M. K. (1994). Mud volcanism in the Mediterranean and Black Sea and shallow structure of the Eratostene seamount. *UNESCO Rep. Mar. Sci., 64*, 173.

Loher M., Pape T., Marcon Y., Römer M., Wintersteller P., Praeg D., Torres M., Sahling H., Bohrmann G. (2018). Mud extrusion and ring-fault gas seepage – upward branching fluid discharge at a deep-sea mud volcano. *Scientific Reports, 8* (6275).

López-Rodríguez C., De Lange G. J., Comas M., Martínez-Ruiz F., Nieto F, Sapart C. J., Mogollón J. M. (2019). Recent, deep-sourced methane/mud discharge at the most active mud volcano in the western Mediterranean. *Marine Geology, 408*, 1–17.

Lykousis V., Alexandri S., Woodside J., de Lange G., Dählmann A., Perissoratis C., Heeschen K., Ioakim C., Sakellariou D., Nomikou P., Rousakis G., Casas D., Ballas D., Ercilla G. (2009). Mud volcanoes and gas hydrates in the Anaximander mountains (Eastern Mediterranean Sea). *Mar. Petrol. Geol*., 26, 854–872.

Mabry J., Lan T., Burnard P., Marty B. (2013). High-precision helium isotope measurements in air. *J. Anal. At. Spectrom. 28*, 1903. doi:10.1039/c3ja50155h

Mamyrin B. A. and Tolstikhin I. N. (1984). Helium isotopes in nature. New York: Elsevier, pp. 273.

Marty B., Jambon A., Sano Y. (1989). Helium isotopes and CO2 in volcanic gases of Japan. *Chem. Geol., 76*, 25-40.

Mascle J., Mary F., Praeg D., Brosolo L., Camera L., Ceramicola S., Dupré S. (2014). Distribution and geological control of mud volcanoes and other fluid/free gas seepage features in the Mediterranean Sea and nearby Gulf of Cadiz. *Geo-Marine Letters, 34* (2-3), 89-110.

Mauffret A., Contrucci I., Brunet C. (1999). Structural evolution of the Northern Tyrrhenian Sea from new seismic data. *Mar. Petrol. Geol., 16*, 381–407.

Mazzini A., Svensen H., Planke S., Guliyev I., Akhmanov G.G., Fallik T., Banks D. (2009). When mud volcanoes sleep: Insight from seep geochemistry at the Dashgil mud volcano, Azerbaijan. *Marine and Petroleum Geology, 26*, 1704–1715.

Mazzini A., Etiope G. (2017). Mud volcanism: an updated review. *Earth-Science Reviews, 168*, 81-112.

Meister P., Wiedling J., Lott C., Bach W., Kuhfuß H., Wegener G., Böttcher M. E., Deusner C., Lichtschlag A., Bernasconi S. M., Weber M. (2018). Anaerobic methane oxidation inducing carbonate precipitation at abiogenic methane seeps in the Tuscan Archipelago (Italy). *PLoS One*, *13*.

Milkov A.V. (2000). Worldwide distribution of submarine mud volcanoes and associated gas hydrates. *Mar. Geol., 167*, 29–42.

Milkov A.V., Sassen R., Apanasovich T. V., Dadashev F. G. (2003). Global gas flux from mud volcanoes: A significant source of fossil methane in the atmosphere and the ocean. *Geophys. Res. Lett., 30* (2), 1037.

Milkov A.V., 2018. Secondary microbial gas. In: Wilkes, H. (Ed.), Hydrocarbons, Oils and Lipids: Diversity, Origin, Chemistry and Fate. Handbook of Hydrocarbon and Lipid Microbiology. Springer, Cham.

Milkov A. V. and Etiope G. (2018). Revised genetic diagrams for natural gases based on a global dataset of >20,000 samples. *Organic Geochemistry, 125*, 109-120.

Morrison and Pine (1955). Radiogenic Origin of the Helium Isotopes in Rock. *Annals of the New York Academy of sciences, 62* (3), 71-92.

Motteran G. and Ventura G. (2005). Aspetti geologici, morfologici e ambientali dello scoglio d'africa (arcipelago toscano): nota preliminare. *Atti Soc. tosc. Sci. nat., Mem., Serie A, 110*, 51-60.

Niemann H. and Boetius A. (2010). Mud volcanoes. In Timmis K. M. (eds). *Handbook of Hydrocarbon and Lipid Microbiology* (pp. 205-214). Berlin Heidelberg: Springer.

Nuzzo M., Tomonaga Y., Schmidt M., Valadares V., Faber E., Pinero E., Reitz A., Haeckel M., Tyroller L., Godinho E., Kipfer R., Terrinha P. G., Hensen C. (2019). Formation and migration of hydrocarbons in deeply buried sediments of the Gulf of Cadiz convergent plate boundary - Insights from the hydrocarbon and helium isotope geochemistry of mud volcano fluids. *Marine Geology, 410*, 56–69.

Ozima M. and Podosek F. A. (2002). Noble Gas Geochemistry (2nd edition). Cambridge, UK: Cambridge University Press, pp. 286.

Palmer R.M., Spivack A. J. and Edmond J. M. (1987). Temperature and pH controls over isotopic fractionation during adsorption of boron on marine clay. *Geochimica et Cosmochimica Acta, 51*, 2319–2323.

Pandeli E., Principi G., Bortolotti V., Benvenuti M., Fazzuoli M., Dini A., Fanucci F., Menna F., Nirta G. (2013). The Elba Island: an intriguing geological puzzle in the Northern Thyrrenian Sea. *Geological Field Trips, 5* (2.1).

Pascucci V., Merlini S., Martini I. P. (1999). Seismic stratigraphy of the Miocene-Pleistocene sedimentary basins of the northern Tyrrhenian Sea and western Tuscany (Italy). *Basin Research, 11*, 337-356.

Rabaute A. and Chamote-Rooke N. (2007). Quantitative mapping of active mud volcanism at the western Mediterranean Ridge-backstop contact. *Mar. Geophys. Res., 28*, 271-295.

Romano E., Ausili A., Bergamin L., Celia Magno M., Pierfranceschi G., Venti F., 2018. Analisi granulometriche dei sedimenti marini. Linee Guida SNPA 18/2018.

Ruff S.E., Kuhfuss H., Wegener G., Lott C., Ramette A., Wiedling J., Knittel K., Weber M. (2016). Methane seep in shallow-water permeable sediment harbors high diversity of anaerobic methanotrophic communities, Elba, Italy. *Frontiers in Microbiology, 7* (374).

Sakata S., Sano Y., Maekawa T. and Igari S. I. (1997). Hydrogen and carbon isotopic composition of methane as evidence for biogenic origin of natural gases from the Green Tuff basin, Japan. *Org. Geochem., 26*, 399–407.

Sano Y. and Wakita H. (1985). Geographical distribution of $^{3}He/^{4}He$ ratios in Japan: Implications for arc tectonics and incipient magmatism. *J. Geophys. Res., 90*, 8729-8741.

Sano Y. and Marty B. (1995). Origin of carbon in fumarolic gas from island arcs. *Chem. Geol. (Isot. Geosci. Sect.), 119*, 265-274.

Sano Y. and Williams S. (1996). Fluxes of mantle and subducted carbon along convergent plate boundaries. *Geophysical Research Letters*, *23* (20), 2749-2752. https://doi.org/10.1029/96GL02260

Sano Y., Tokutake T., Takahata N. (2008). Accurate measurement of atmospheric helium isotopes. *Anal. Sci., 24*, 521-525.

Sano Y., Kinoshita N., Kagoshima T. et al. (2017). Origin of methane-rich natural gas at the West Pacific convergent plate boundary. *Sci. Rep., 7*, 15646.

Schoell M. (1983). Genetic characterization of natural gases. *Am. Assoc. Pet. Geol. Bull., 67*, 2225-2238.

Sciarra A., Saroni A., Etiope G., Coltorti M., Mazzarini F., Lott C., Grassa F., Italiano F. (2019a). Shallow water submarine seep of abiotic methane from serpentinized peridotites off the Island of Elba, Italy. *Appl. Geoch., 100*, 1-7.

Sciarra A., Cantucci B., Ricci T., Tomonaga Y., Mazzini A. (2019b). Geochemical characterization of the Nirano mud volcano, Italy. *Appl. Geoch., 102*, 77-87.

Shepard F. P. (1954). Nomenclature based on sand-silt-clay ratios. *Journal Sedimentary Petrology, 24*, 151-158.

Shuai Y., Zhang S., Peng P., Zou Y., Yuan X., Liu J. (2013). Occurrence of heavy carbon dioxide of organic origin: Evidence from confined dry pyrolysis of coal. *Chemical Geology, 358*, 54-60.

Tassi F., Fiebig J., Vaselli O., Nocentini M. (2012). Origins of methane discharging from volcanic–hydrothermal, geothermal and cold emissions in Italy. *Chemical Geology, 310–311*, 36-48.

Vacquand C., Deville E., Beaumont V., Guyot F., Sissmann O., Pillot D., Arcilla C., Prinzhofer A. (2018). Reduced gas seepages in ophiolitic complexes: evidences for multiple origins of the H_2-CH_4-N_2 gas mixtures. *Geochem. Cosmochim. Acta 233*, 437–461.

Yang, T.F., Chen, C.H., Tien, R.L., Song, S.R., Liu, T.K. (2003). Remnant magmatic activity in the coastal range of east Taiwan after arc-continent collision: fissiontrack data and $^{3}He/^{4}He$ ratio evidence. *Radiat. Meas., 36*, 343–349.

Wakita H., Sano Y., Urabe A. and Nakamura Y. (1990). Origin of methane-rich natural gas in Japan: formation of gas fields due to large-scale submarine volcanism. *Appl. Geochem., 5*, 263–278.

Whiticar M.J., Faber E. and Schoell M. (1986). Biogenic methane formation in marine and freshwater environments: CO_2 reduction vs. acetate fermentation — isotope evidence. *Geochimica et Cosmochimica Acta, 50*, 693-709. http://dx.doi.org/10.1016/0016-7037(86)90346-7.

Whiticar M.J. (1999). Carbon and hydrogen isotope systematics of bacterial formation and oxidation of methane. *Chemical Geology, 161,* 291-314.

Wiedling J. (2010). Biogeochemical investigations on a shallow water methane seep in the Mediterranean Sea. Bachelor Thesis, Greifswald University.

Zheng G., Ma X., Z. Guo, Hilton D. R., Xu W., Liang S., Fan Q., Chen W. (2017). Gas geochemistry and methane emission from Dushanzi mud volcanoes in the southern Junggar Basin, NW China. *Journal of Asian Earth Sciences, 149,* 184–190.

Zitter T.A.C., Huguen C., Woodside J. M. (2005). Geology of mud volcanoes in the eastern Mediterranean from combined sidescan sonar and submersible surveys. *Deep-Sea Research I, 52,* 457-475.

Figure captions

Figure 1 *– Bathymetric map of the area between the island of Elba and Montecristo showing the location of Scoglio d'Affrica, Pomonte and Pianosa emission sites. In the inset, locations of the Scoglio d'Affrica emission activities detected in 2011, 2017 and 2018 are shown. In 2011 the HYDRA Institute investigated the mud volcano near Scoglio d'Affrica at 8-10 meters of water depth. The area was about 15 by 5 meters large with three gas emissions and some emissions in between the rocks in crevices around the mud volcano (HYDRA Institute, 2011; Meister et al. 2018). On the 16th March 2017, local fishermen reported a column of muddy water of 10 m height gushing out from the sea surface in an area located south of the site explored in 2011. The Italian Protezione Civile investigated the area and found gas emission spots predominant in shallow water (8-10 m), sometimes inconstant and without temperature anomalies. Some of these seeps were N-S aligned with* CH_4 *and* CO_2 *concentration anomalies (Chiocci et al., 2017).*

Figure 2 *– Photo mosaic of the emission area in 2018 at Scoglio d'Affrica mud volcano. At least 10 sites of emission are recognizable. The inset shows the geolocation of the photo mosaic. The shoal to the south-east of the photo mosaic is the site related to the emission activity detected in 2017. For higher resolution image, see figure 2S in the Supplementary Material.*

Figure 3 *– Scoglio d'Affrica mud volcano in 2018. A, B: mud mound corresponding to emission point 7 in figure 2. C: bubbles emission corresponding to point 3 in figure 2. D: view of the mud volcano area from point 5 of figure 2.*

Figure 4 *– A: granulometric composition of samples S2, S4-5 and S8 in Shepard's diagram (1954). B: granulometric composition of sample S4 in Shepard's diagram modified as in Romano et al. (2018).*

Figure 5 – *A, B, C: Scoglio d'Affrica mud volcano 2018 gas (SdA MV 2018) compared with 2011 (Meister at al., 2018) and Pomonte gases (Sciarra et al., 2019a), together with other MVs gases from literature, inserted into the revised genetic diagrams from Milkov and Etiope (2018). A:* $CH_4/(C_2H_6+C_3H_8)$ *ratio versus* $\delta^{13}C$-CH_4 *diagram comparing gases from Scoglio d'Affrica MV (2018), Pomonte seeps, Venere MV (Loher et al. 2018; Blumenberg M., 2018), Ginsburg MV and Mercator MV (Nuzzo et al., 2019). Venere MV is an offshore mud volcano, located in the Ionian Sea at 1600 m water depth. The molecular and isotopic composition of the methane emitted from this mud volcano reveals a thermogenic origin, as also Loher et al. (2018) and Blumenberg et al. (2018) reported. Mercator and Ginsburg MVs are at ~900 m water depth in the Gulf of Cadiz and fit thermogenic values in the genetic diagrams. B:* $\delta^{13}C$-CO_2 *versus* $\delta^{13}C$-CH_4 *diagram comparing gases from Scoglio d'Affrica MV (2011 and 2018), Pomonte seeps and Nirano MV (Sciarra et al., 2019b). Nirano MV is located onshore, in the western sector of the Modena Apennine margin (Italy), upon an anticline structure associated to the Pede-Apennines thrust (Sciarra et al., 2019b). C:* $\delta^{13}C$-CH_4 *versus* $\delta^{2}H$-CH_4 *diagram comparing gases from Scoglio d'Affrica MV (2018), Pomonte seeps, Carmen MV (Lopez et al., 2019), Venere MV, Mercator MV and Ginsburg MV. Carmen MV is located in the westernmost part of Mediterranean Sea, in the Alboran Basin, that consists of Miocene to Quaternary sedimentary sequences of up to 8 km in thickness. Carmen MV extends for 65 m in height and 1 km in diameter (Lopez et al., 2019): CR – CO2 reduction, F – methyl-type fermentation, SM – secondary microbial, EMT – early mature thermogenic gas, OA – oil-associated thermogenic gas, LMT – late mature thermogenic gas.*

Figure 6 *– Stable carbon and hydrogen isotope ratios of methane in Scoglio d'Affrica mud volcano compared to other gases compositions from conventional petroleum systems and serpentinized peridotites. The diagram compares methane of biotic and abiotic origins: small dots refer to biotic (microbial and thermogenic) gas in sedimentary basins (from unpublished global data-sets; see Etiope and Schoell, 2014 and references therein), whereas triangles refer to gas from serpentinization processes (from Etiope, 2017;*

Etiope et al., 2017 and references therein, with additional data from Vacquand et al., 2018). The gases from Scoglio d'Affrica MV fit the range of biotic origin, whereas Pomonte-Elba samples fit the range of abiotic origin.

***Figure 7** – A: $^{3}He/^{4}He$ versus $^{4}He/^{20}Ne$ diagram showing crustal-/mantle-derived helium contribution; B: $CH_4/^{3}He$ ratio versus $\delta^{13}C\text{-}CH_4$ diagram comparing gases from Scoglio d'Affrica MV (2018) and Pomonte seeps. Four end members are considered: (1) biogenic methane produced by chemical reactions, as observed on the East Pacific Rise (EPR); (2) biogenic methane produced by microbial activity utilizing inorganic carbon; (3) thermogenic methane from the thermal decomposition of organic matter; and (4) oxidized methane with heavier carbon isotope values formed through microbial fractionation in old gas plumes.*

***Figure 8** – Synthetic stratigraphy of the two wells Mimosa 1 and Martina 1, showing the unconformity bounded units. Main seismic unconformities (after Cornamusini et al., 2002): X at the base of the Unit Sub2; A at the base of the Unit Lit0; D at the base of the Unit Lit7 (from Cornamusini and Pascucci, 2014).*

Tab. 1 – Gas analysis results.

ID	He (ppmv)	CO (ppmv)	N_2 (vol%)	CH_4 (vol%)	CO_2 (vol%)	C_2H_6 (vol%)	$\delta^{13}C_{CO2}$ (VPDB)	$\delta^{13}C_{CH4}$ (VPDB)	$\delta^{2}H_{CH4}$ (VSMOW)	$^{3}He/^{4}He$ (R_c/R_a)	$^{4}He/^{20}Ne$	C_1/C_2+C_3	$C_{CH4}/^{3}He$
GG2	42	1.30	0.70	96.05	1.30	0.036	15.5	-35.0	-163	0.01	317.43	2676	$1{,}76 \cdot 10^{12}$
GG3	44	1.10	0.84	95.50	1.10	0.026	15.3	-36.4	-167	0.01	329.92	3687	$1{,}76 \cdot 10^{12}$
GG5	44	b.d.l.	0.41	96.82	1.18	0.030	15.6	-36.8	-168	0.01	172.24	3249	$1{,}45 \cdot 10^{12}$
GG6	46	0.60	0.72	96.75	0.97	0.036	21.7	-34.9	-165	0.01	75.15	2718	$1{,}24 \cdot 10^{12}$

H_2 and propane (C_3H_8) are below detection limits in all samples.

Tab. 2 – Extruded sediment samples.

Sample ID	Point of sampling	Depth of sampling from the sea bottom	Shepard's classification
S4	Mud volcano point 4	Superficial sediment	Gravelly mud
S8	Mud volcano point 8	0 - 5 cm depth	Silty clay
S2	Mud volcano point 2	20 - 30 cm depth	Silty clay
S4-5	No more active mud volcano between point 4 and 5	Superficial sediment	Sand-silt-clay (loam)

Figure 1

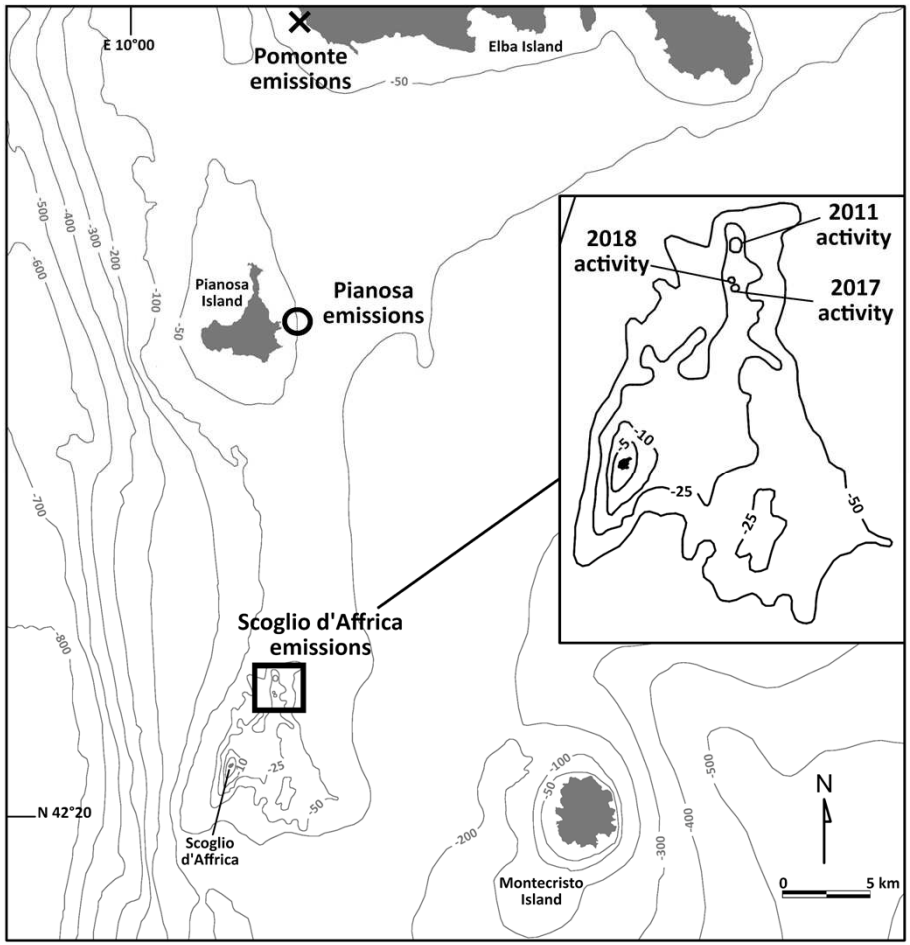
E 10°00
Pomonte
emissions
Elba Island
-50
-500
-400
-300
-200
-100
-50
-600
Pianosa
Island
Pianosa
emissions
-700
-800
2018
activity
2011
activity
2017
activity
-5
-10
-25
-50
-25
Scoglio d'Affrica
emissions
-10
-25
-50
N 42°20
Scoglio
d'Affrica
-200
-100
-50
-300
-400
-500
Montecristo
Island
N
0
5 km

Figure 2

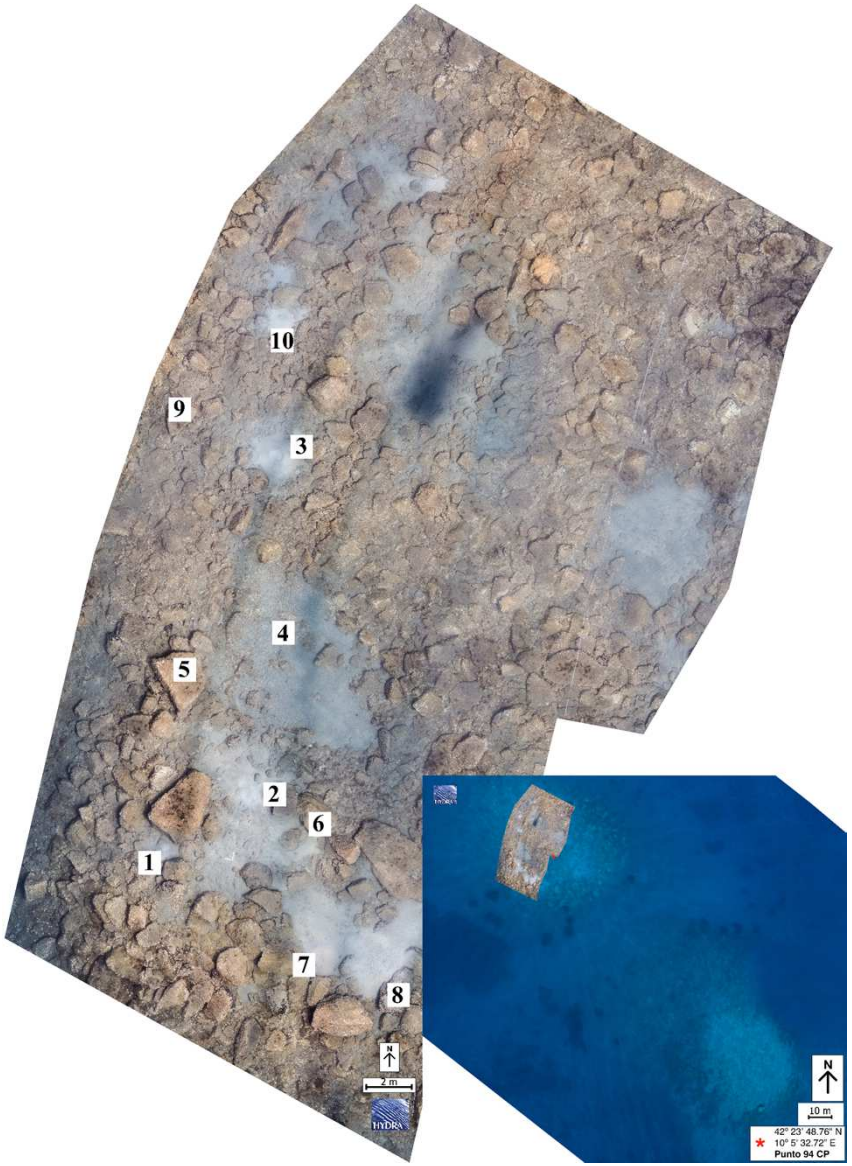

Figure 3

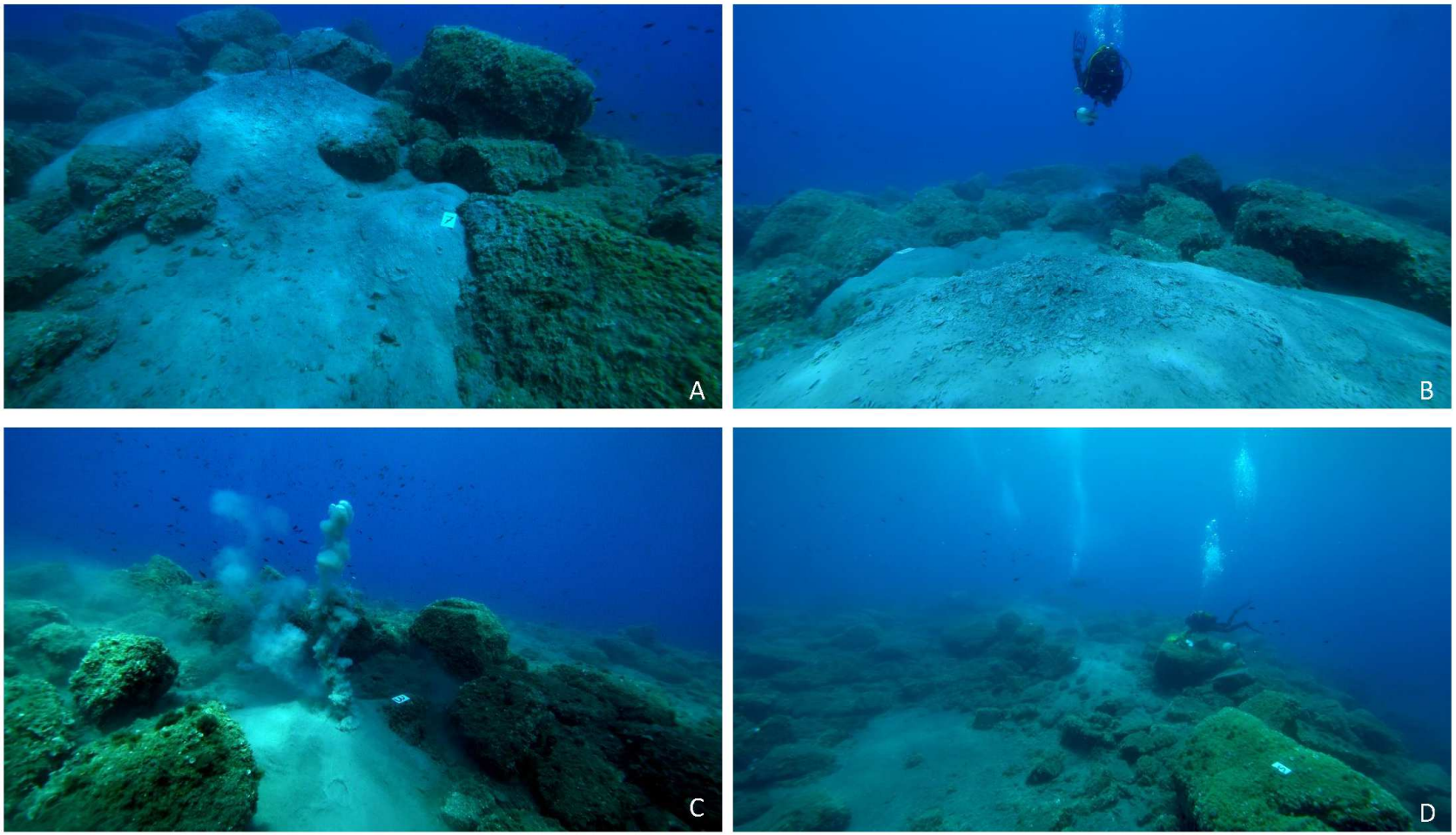

Figure 4

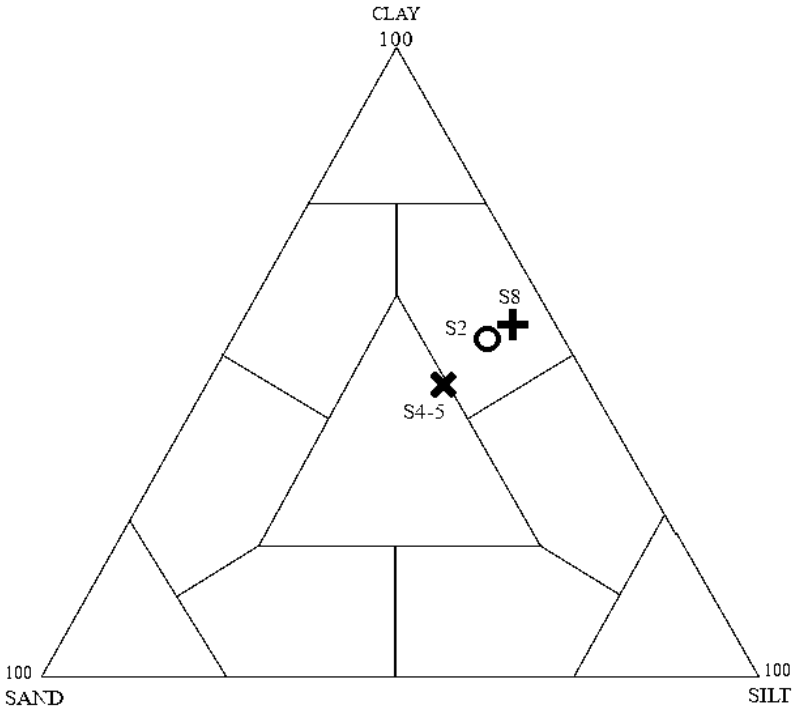
CLAY
100
S8
S2
S4-5
100
SAND
100
SILT

A

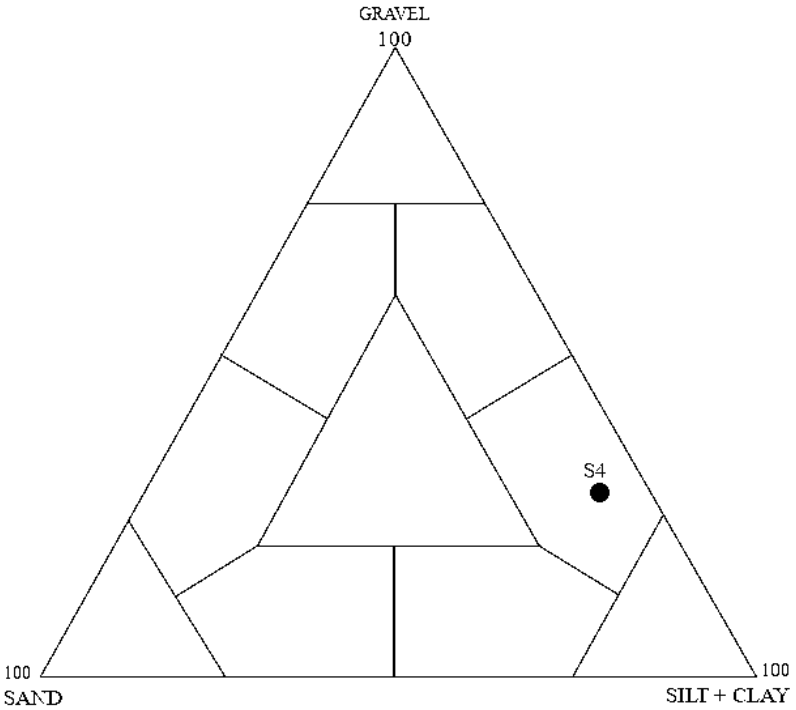
GRAVEL
100
S4
100
SAND
100
SILT + CLAY

B

Figure 5

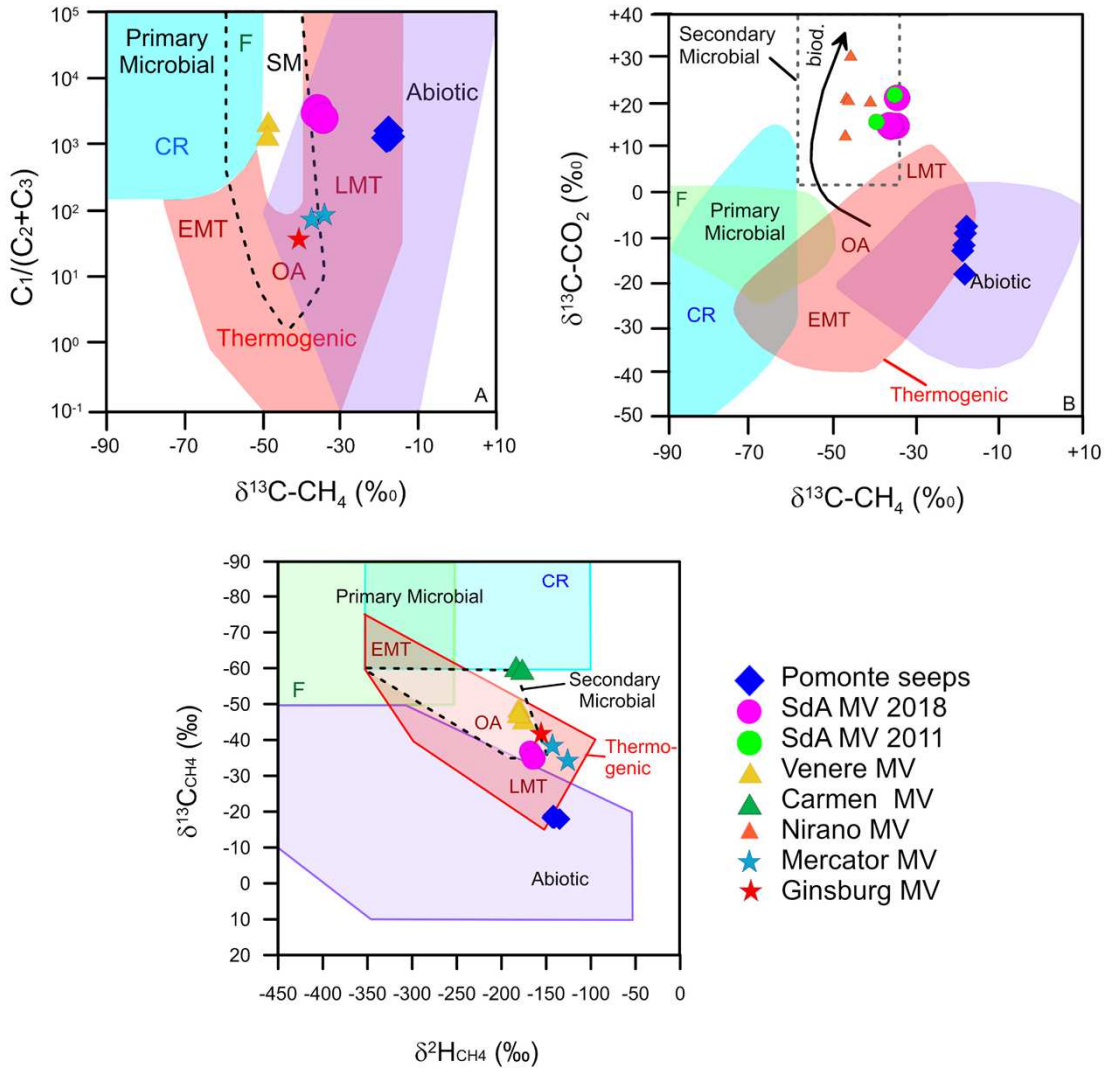
Primary Microbial
F
SM
Abiotic
CR
LMT
EMT
OA
Thermogenic
A
C1/(C2+C3)
δ13C-CH4 (‰)
Secondary Microbial
biod.
LMT
F
Primary Microbial
OA
Abiotic
CR
EMT
Thermogenic
B
δ13C-CO2 (‰)
δ13C-CH4 (‰)
Primary Microbial
CR
EMT
Secondary Microbial
F
OA
Thermo-genic
LMT
Abiotic
δ13CCH4 (‰)
δ2HCH4 (‰)
Pomonte seeps
SdA MV 2018
SdA MV 2011
Venere MV
Carmen MV
Nirano MV
Mercator MV
Ginsburg MV

Figure 6

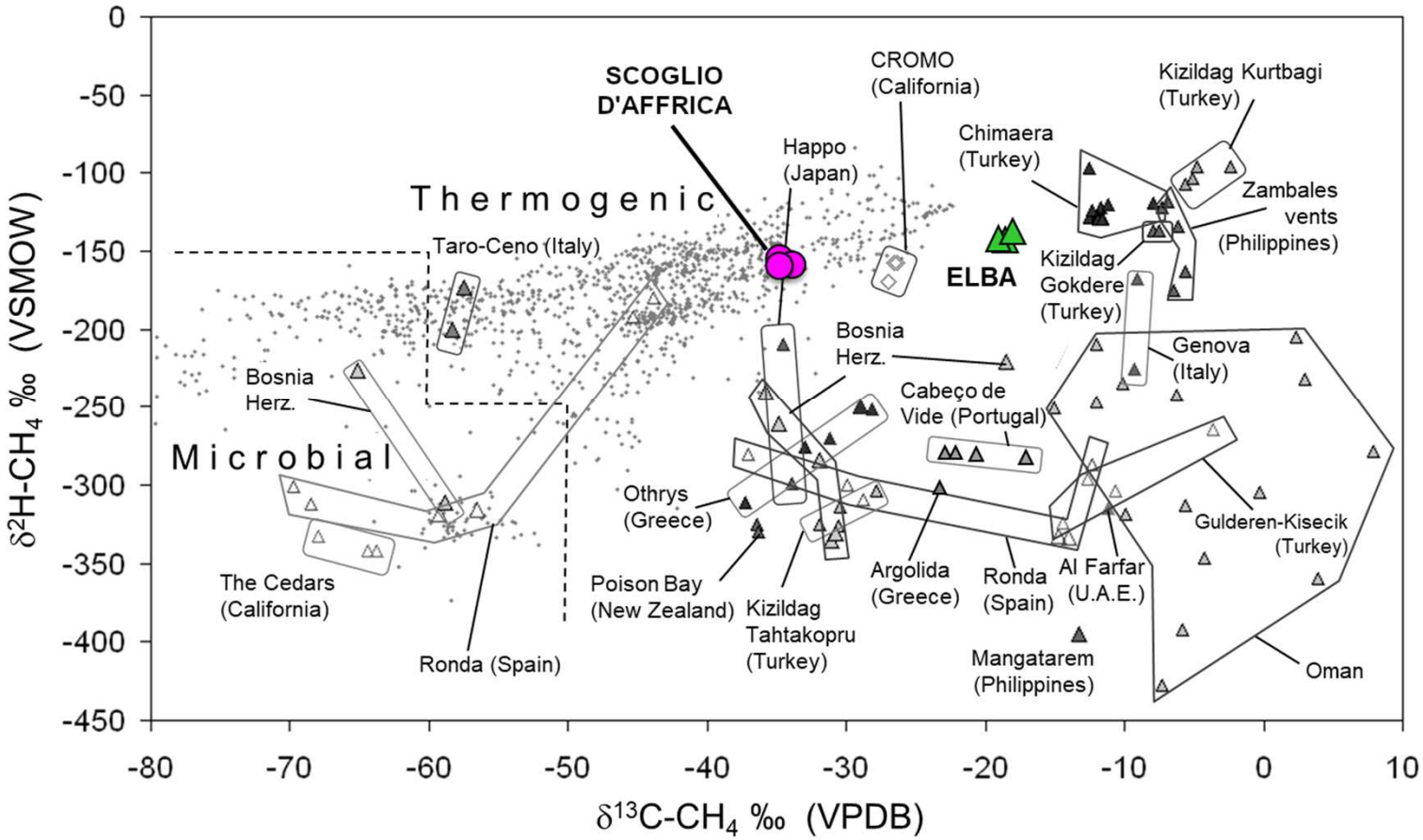
SCOGLIO D'AFFRICA
CROMO (California)
Kizildag Kurtbagi (Turkey)
Chimaera (Turkey)
Happo (Japan)
Thermogenic
Zambales vents (Philippines)
Taro-Ceno (Italy)
ELBA
Kizildag Gokdere (Turkey)
Bosnia Herz.
Genova (Italy)
Bosnia Herz.
Cabeço de Vide (Portugal)
Microbial
Othrys (Greece)
Gulderen-Kisecik (Turkey)
The Cedars (California)
Poison Bay (New Zealand)
Kizildag Tahtakopru (Turkey)
Argolida (Greece)
Ronda (Spain)
Al Farfar (U.A.E.)
Ronda (Spain)
Mangatarem (Philippines)
Oman
δ2H-CH4 ‰ (VSMOW)
δ13C-CH4 ‰ (VPDB)
0
-50
-100
-150
-200
-250
-300
-350
-400
-450
-80
-70
-60
-50
-40
-30
-20
-10
0
10

Figure 7

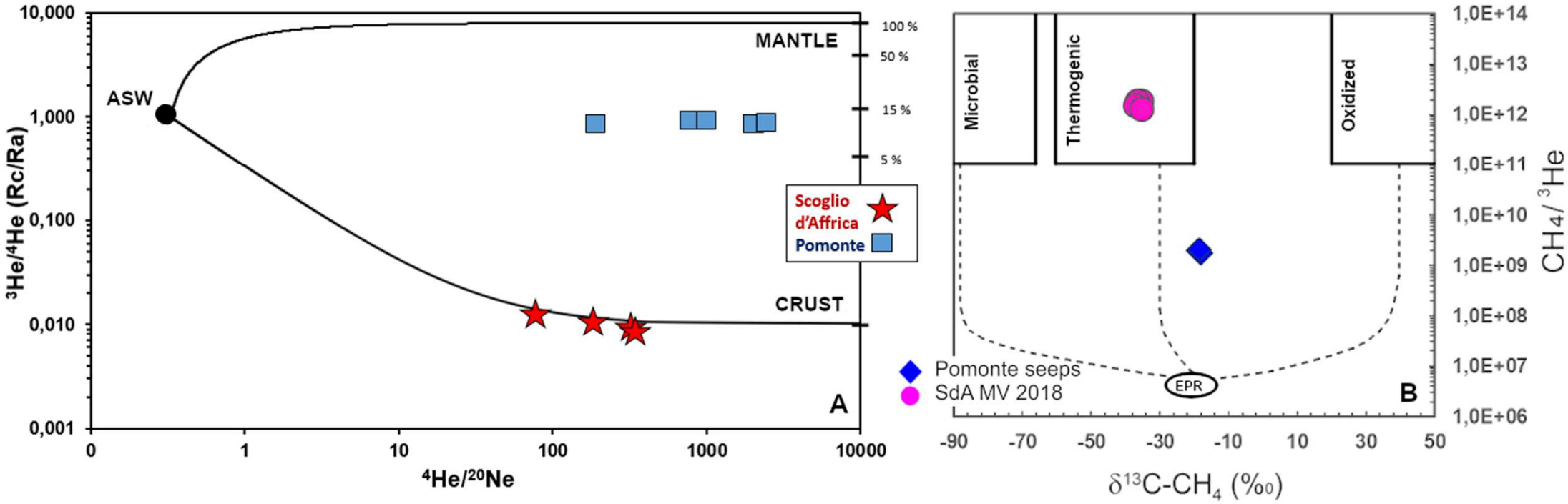
10,000
1,000
0,100
0,010
0,001
^{3}He/^{4}He (Rc/Ra)
0
1
10
100
1000
10000
^{4}He/^{20}Ne
ASW
MANTLE
CRUST
100 %
50 %
15 %
5 %
Scoglio d'Affrica
Pomonte
A
Microbial
Thermogenic
Oxidized
EPR
Pomonte seeps
SdA MV 2018
B
-90
-70
-50
-30
-10
10
30
50
δ^{13}C-CH$_4$ (‰)
1,0E+14
1,0E+13
1,0E+12
1,0E+11
1,0E+10
1,0E+09
1,0E+08
1,0E+07
1,0E+06
CH$_4$/^{3}He

Figure 8

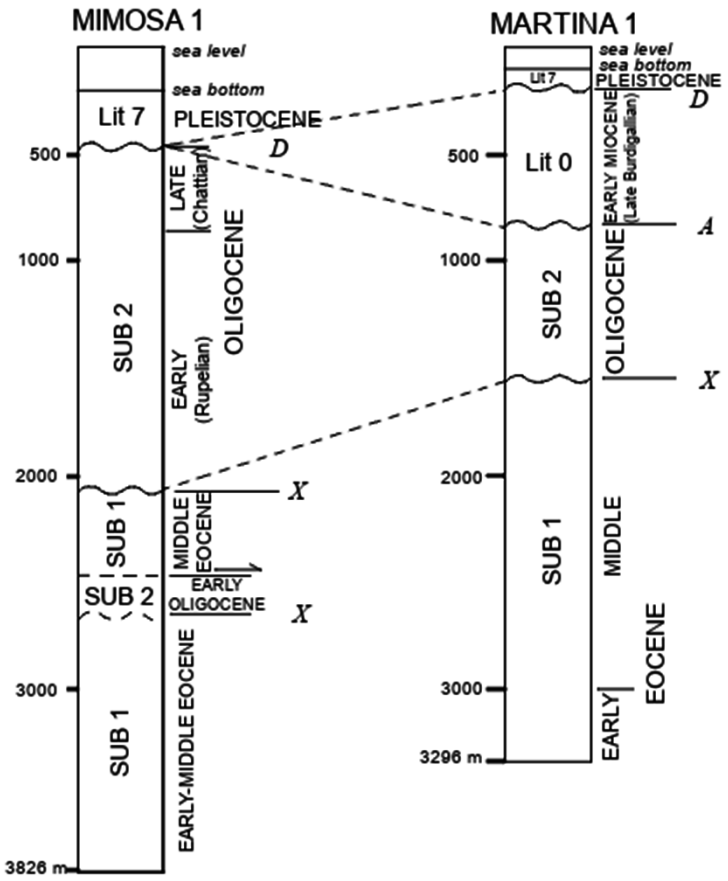
MIMOSA 1
sea level
sea bottom
Lit 7
PLEISTOCENE
D
500
1000
SUB 2
LATE (Chattian)
OLIGOCENE
EARLY (Rupelian)
2000
X
SUB 1
MIDDLE EOCENE
EARLY OLIGOCENE
SUB 2
X
3000
SUB 1
EARLY-MIDDLE EOCENE
3826 m
MARTINA 1
sea level
sea bottom
Lit7
PLEISTOCENE
D
500
Lit 0
EARLY MIOCENE (Late Burdigalian)
A
1000
SUB 2
OLIGOCENE
X
2000
SUB 1
MIDDLE
3000
EARLY
EOCENE
3296 m

- A photo-mosaic of the shallowest mud volcano in the Tyrrheanian Sea is reported
- Analysis of isotopic and molecular composition of submarine methane emissions
- Carbon dioxide is enriched in heavy carbon isotopes
- Radiogenic crustal helium reveals discontinuities in shallow crustal levels
- Secondary microbial origin is predominant; abiotic origin is discarded

Declaration of interests

☒ The authors declare that they have no known competing financial interests or personal relationships that could have appeared to influence the work reported in this paper.

☐The authors declare the following financial interests/personal relationships which may be considered as potential competing interests: